Evolution of Displacement Speed Statistics during Flame-Wall Interaction within Turbulent Boundary Layers

Gulcan Ozel-Erol[1], Umair Ahmed[2], Nilanjan Chakraborty[2]
[1]Department of Mechanical Engineering, Bilecik Seyh Edebali University
Bilecik, Turkey
[2]School of Engineering, Newcastle University
Newcastle-Upon-Tyne, United Kingdom

1 Introduction

The speed with which a premixed flame surface propagates normal to itself with respect to an initially coincident material surface is known as the displacement speed S_d. Several previous studies (see [1-4] and references therein) concentrated on the statistics of displacement speed S_d of turbulent premixed flames along with its strain rate and curvature dependencies because of its importance in level-set [5] and Flame Surface Density [6] based methodologies of turbulent premixed combustion modelling. Previous analyses on flame displacement speed statistics in premixed flames have been conducted for combustion processes occurring without the influence of boundary layers which form due to the existence of walls. However, this aspect is yet to be addressed in the case for flame-wall interaction (FWI). Modern combustors are made smaller in size to increase power-density and make them compatible with electrical powertrain and FWI occurs more readily in these small-sized combustors than in conventional combustors.

The statistical behaviour of the flame displacement speed S_d is determined by the imbalance between chemical reaction rate and molecular diffusion rate, and also by the reactive scalar gradient magnitude [1-4]. It has been demonstrated by Ahmed et al. [7] that the molecular diffusion rate and reactive scalar gradient are affected by the shear rate induced by the presence of wall and the boundary condition prevailing there. Thus, it is expected that the statistical behaviour of displacement speed and its local strain rate and curvature dependence are affected by the presence of the wall during FWI. Moreover, the effects of wall boundary condition on flame displacement speed statistics are yet to be analysed in detail. The aforementioned gaps in the existing literature will be addressed in this analysis by using a three-dimensional Direct Numerical Simulations (DNS) database of head-on interaction (HOI) of statistically planar flames propagating across turbulent boundary layers [8,9]. Two different wall boundary conditions, namely, isothermal, and adiabatic walls, have been considered in this analysis to investigate the influence of wall boundary condition on displacement speed statistics at different stages of FWI. It is worth noting that HOI across a turbulent boundary layer is an unsteady event and thus the displacement speed statistics will be presented at time instants when the flame is at different distances from the wall and therefore at different stages of FWI. Thus, the main objectives of the present analysis are: (a) to analyse the statistical behaviour of displacement speed and its curvature and strain

Correspondence to: gulcan.ozel@bilecik.edu.tr

rate dependences at different stages of FWI, (b) to demonstrate and explain the influence of wall boundary condition on the aspects described in (a).

2 Mathematical Background and Numerical Implementation

In premixed flames a reaction progress variable c can be defined based on a suitable major species mass fraction Y as: $c = (Y_0 - Y)/(Y_0 - Y_\infty)$ with subscripts 0 and ∞ referring to values in unburned gas and fully burned products, respectively. The transport equation of c takes the following form:

$$\rho(\partial c/\partial t + u_j\, \partial c/\partial x_j) = \dot{w} + \nabla \cdot (\rho D \nabla c) \quad (1)$$

Here, ρ, u_j, D and $\dot{w}$ are gas density, j[th] component of fluid velocity, progress variable diffusivity and reaction rate of progress variable, respectively. Equation 1 can be written in the kinematic form for a given c-isosurface in the following manner:

$$\left[\partial c/\partial t + u_j\, \partial c/\partial x_j\right] = S_d|\nabla c| \quad (2)$$

where S_d is the displacement speed, which can be expressed in the following manner [1-4]:

$$S_d = [\dot{w} + \nabla \cdot (\rho D \nabla c)]/\rho|\nabla c| = S_r + S_n + S_t \quad (3)$$

Here, S_r, S_n and S_t are the reaction, normal diffusion and tangential components of displacement speed, which are given as [1-4]:

$$S_r = \dot{w}/\rho|\nabla c|\,;\; S_n = \vec{N} \cdot \nabla \cdot (\rho D \vec{N} \cdot \nabla c)/\rho|\nabla c| \text{ and } S_t = -2D\kappa_m \quad (4)$$

where $\vec{N} = -\nabla c/|\nabla c|$ is the flame normal vector and $\kappa_m = 0.5\nabla \cdot \vec{N}$ is the local flame curvature. According to the current convention, the flame normal vector points towards the reactants and the flame surface convex (concave) towards the reactants has a positive (negative) curvature.

It can be seen from eqs. 3 and 4 that the gas density ρ affects the displacement speed and its components and thus it is worthwhile to consider the density-weighted displacement speed $S_d^* = \rho S_d/\rho_0$ and its components: $S_r^* = \rho S_r/\rho_0$, $S_n^* = \rho S_n/\rho_0$ and $S_t^* = \rho S_t/\rho_0$ where ρ_0 is the unburned gas density. Moreover, S_d^* plays a key role in terms of modelling turbulent premixed combustion [6]. The statistics of S_d^*, S_r^*, S_n^* and S_t^* will be presented at different stages of HOI of statistically planar flames across turbulent boundary layers using DNS data.

The simulations used for this analysis have been carried out using a three-dimensional code called SENGA+ [3-4,6], which employs a 10[th] order central-difference scheme for approximating the spatial gradients for the internal grid points, but the order of accuracy gradually reduces to second order for the non-periodic boundaries. The time-advancement is accounted for by a low storage third order Runge-Kutta scheme. A single-step irreversible Arrhenius type chemical reaction for stoichiometric methane-air combustion (unit mass of Fuel + s unit mass of Oxidiser → (1+s) unit mass of Products, where $s = 4.0$ is the stoichiometric oxidiser-fuel mass ratio for methane-air mixture) is considered for the current analysis. The unburned gas temperature T_0 is considered to be 730K, which yields a heat release rate parameter of $\tau = (T_{ad} - T_0)/T_0 = 2.3$. The Lewis number of all the species is taken to be unity for the sake of simplicity, and standard values are considered for the Prandtl number Pr and the ratio of specific heat, γ (i.e., $Pr = 0.7, \gamma = 1.4$). Several previous studies demonstrated that the statistics of reactive scalar gradient [10], displacement speed [4], maximum wall heat flux magnitude [10] and the flame quenching distance [10] from simple chemistry are in good agreement with the corresponding results obtained from detailed chemistry. Thus, the simplification of chemistry is unlikely to affect the qualitative nature of the conclusions of this analysis.

The configuration which has been employed for this analysis considers turbulent boundary layer on top of a chemically inert wall, and the initial flow condition is specified using a non-reacting fully developed turbulent channel flow solution corresponding to $Re_\tau = \rho_0 u_{\tau,NR} h/\mu_0 = 110$ where μ_0 is the unburned gas viscosity and h is the channel half height. The simulation domain size of

$10.69h \times 1.33h \times 4h$ is discretised by an equidistant grid $1920 \times 240 \times 720$, which ensures at least 8 grid points within the thermal flame thickness $\delta_{th} = (T_{ad} - T_0)/\max|\nabla T|_L$ for $S_L/u_{\tau,NR} = 0.7$ with S_L, $u_{\tau,NR} = \sqrt{|\tau_{w.NR}|/\rho}$ and $\tau_{w,NR}$ are the unstretched laminar burning velocity, friction velocity and wall shear stress for the non-reacting channel flow, respectively. The longitudinal integral length scale L_{11} and root-mean-square turbulent velocity u' remain of the order of h and $u_{\tau,NR}$, respectively for the channel flow with $Re_\tau = 110$ [11]. This leads to a Damköhler number $Da = L_{11}S_L/u'\delta_{th}$ of 15.80 and a Karlovitz number $Ka = (u'/S_L)^{3/2}(L_{11}/\delta_{th})^{-1/2}$ of 0.36, which suggests that the flame away from the wall is expected to show the attributes of the corrugated flamelets regime combustion [5]. For these simulations, periodic boundary conditions are imposed for the streamwise (i.e. $x-$direction) and spanwise (i.e. $z-$direction) directions and the mean pressure gradient (i.e., $-\partial p/\partial x = \rho u_{\tau,NR}^2/h$ where p is the pressure) is imposed in the streamwise flow direction. Further information can be found in [9] regarding the validation of the non-reacting channel flow simulation, which are not repeated here for the sake of brevity. In the wall-normal direction (i.e. y-direction), a no-slip boundary condition is implemented at $y = 0$, and the temperature is imposed (i.e. $T_w = T_0$) for isothermal wall boundary conditions. For the adiabatic wall boundary condition, a Neumann boundary condition, given by $\partial T/\partial y = 0$ is specified at the wall. At $y/h = 1.33$, the boundary is taken to be partially non-reflecting. A steady freely propagating 1D laminar flame simulation is interpolated to the 3D grid in such a manner that $c = 0.5$ is obtained at $y/h \approx 0.85$ so that the reactant side of the flame faces the wall and the product side of the flame faces towards the outflow side of the boundary in the $y-$direction. The simulations have been continued for 2.0 flow through times based on the maximum mean streamwise velocity given by $21.30u_{\tau,NR}$. The flames interact with the wall within this simulation duration, but the turbulent boundary layer does not evolve significantly during the simulation [8,9].

3 Results and Discussion

The instantaneous views of the $\theta = (T - T_0)/(T_{ad} - T_0) = 0.8$ isosurface at different time instants are shown in Fig. 1 for HOI within turbulent boundary layer for both isothermal and adiabatic wall boundary conditions where $t_f = \delta_{th}/S_L$ is the chemical timescale. The time instants shown in Fig. 1 are representative of the situations (i) when the flame was away from the wall (e.g., $t/t_f = 3.99$), (ii) it starts to interact with the wall (e.g., $t/t_f = 10.92$) and (iii) it is at the final stage of flame quenching (e.g. $t/t_f = 13.12$). This can be substantiated from the probability density functions (PDFs) of the normalised wall-normal distance $\Delta y_{n,wall}/\delta_{th}$ of the $c = 0.8$ isosurface which are shown in Fig. 2 for the time instants described in Fig. 1. The choices of $\theta = 0.8$ and $c = 0.8$ are driven by the fact that the maximum chemical reaction for the freely propagating laminar premixed flame is obtained for these values for the current thermochemistry and thus the $c = 0.8$ isosurface is considered to be the flame surface in this abstract. It can be seen from Fig. 2 that the wall-normal distance of the $c = 0.8$ isosurface decreases with the passage of time for both isothermal and adiabatic boundary conditions. In the case of adiabatic wall boundary condition, the flame eventually extinguishes due to the consumption of reactants when it reaches the wall, which can be seen from the increasingly disappearing $\theta = 0.8$ isosurface in Fig. 1 for this boundary condition. By contrast, in the isothermal boundary condition, the flame quenches due to heat loss through the wall when it reaches close to the wall and the unburned reactants from the vicinity of the wall diffuse to the regions away from the wall, whereas the burned products away from the wall diffuse towards the wall and thus a continuous $\theta = 0.8$ isosurface is obtained due to thermal boundary layer on the isothermal wall. As a consequence, the value of c increases at the wall (i.e. $y = 0$) with the progress of HOI for both isothermal and adiabatic wall boundary conditions and this trend is particularly visible at the late stages of HOI (e.g., $t/t_f = 13.12$). Thus, the differences in near-wall behaviour of $\dot{w}$ between isothermal and adiabatic wall boundary conditions are reflected in the statistics of S_d^* and its components, which will be discussed next.

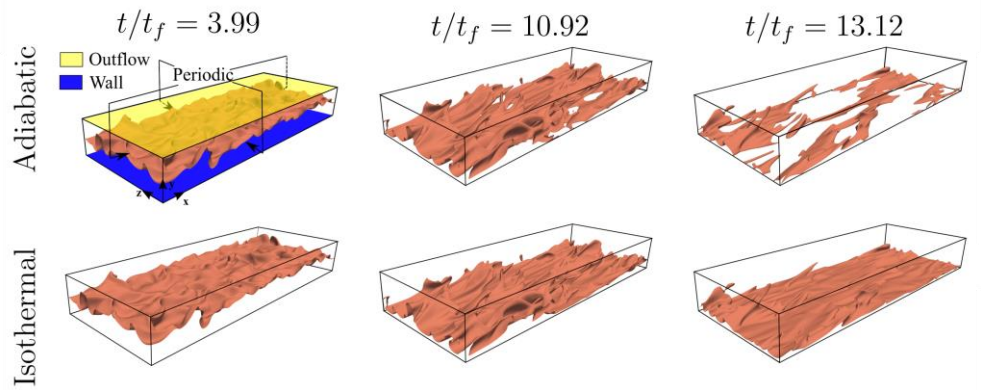

Figure 1: Evolution of $\theta = 0.8$ isosurface with time for adiabatic (top) and isothermal (bottom) walls.

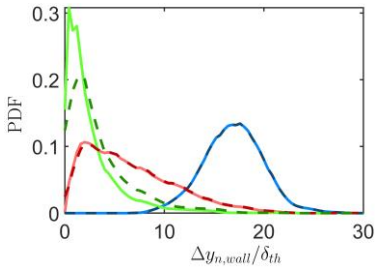

Figure 2: Normal distance of the $c = 0.8$ isosurface to the wall for adiabatic (dashed line) and isothermal (solid line) wall conditions at $t/t_f = 3.99$ (blue), 10.92 (red), 13.12 (green).

The PDFs of S_d^*/S_L and its components (i.e., S_r^*/S_L, S_n^*/S_L and S_t^*/S_L) for the $c = 0.8$ isosurface at different stages of HOI are shown in Fig. 3 for both isothermal and adiabatic wall boundary conditions. It can be seen from Fig. 3 that S_d^* assumes predominantly positive values when the flame remains away from the wall (e.g. $t/t_f = 3.99$) and thus is not affected by its presence. However, the mean value of S_d^*/S_L decreases and the width of the PDF of S_d^*/S_L increases with the progress of FWI. At $t/t_f = 13.12$, when the flame has extensively interacted with the wall, the occurrence of larger values of S_d^*/S_L has greater probability in adiabatic wall case than the isothermal wall boundary condition. To explain this behaviour, it is instructive to examine at the PDFs of S_r^*/S_L, S_n^*/S_L and S_t^*/S_L. It can be seen from Fig. 3 that $S_t^*/S_L = -2D\kappa_m/S_L$ peaks at the zero value and exhibits equal likelihood of positive and negative values for both isothermal and adiabatic boundary conditions because the flames considered here are statistically planar in nature. However, the width of S_t^*/S_L PDFs increases with the progress of FWI as the near wall vortical structures tend to wrinkle the flames more as it comes close to the wall. The components S_r^*/S_L and S_n^*/S_L assume positive and predominantly negative values, respectively at the flame surface, which is consistent with previous analyses [1-4]. It can also be seen from Fig. 3 that the probability of high positive values of S_r^*/S_L in the isothermal wall boundary condition decreases with the progress of HOI and at late times (e.g., $t/t_f = 13.12$) a secondary peak of the S_r^*/S_L PDF is obtained at $S_r^*/S_L = 0$, which is indicative of the flame quenching as a result of wall heat loss. The normal diffusion component S_n^*/S_L can alternatively written as: $S_n^* = -\vec{N} \cdot \nabla(\rho D|\nabla c|)/\rho_0|\nabla c|$, which suggests that the statistical behaviour of $|\nabla c|$ affects the distribution of S_n^*. It has been demonstrated elsewhere [7] that $|\nabla c|$ assumes small values in the near-wall region and interested readers are referred to Ref. [7] where detailed physical explanations were provided. The small values of $|\nabla c|$ in the near-wall region give rise to small magnitudes of flame normal gradient of $|\nabla c|$ (i.e. $|\vec{N} \cdot \nabla(|\nabla c|)|$), which acts to decrease $|S_n^*|$, as the HOI progresses with time.

The combination of decreases in magnitudes of positive S_r^*/S_L and negative S_n^*/S_L acts to reduce the mean value of S_d^*/S_L with the progress of HOI. Moreover, the increased width of S_t^*/S_L PDF as a result

of flame wrinkling induced by near-wall vortical motion acts to increase the width of S_d^*/S_L PDF with the progress of head-on interaction.

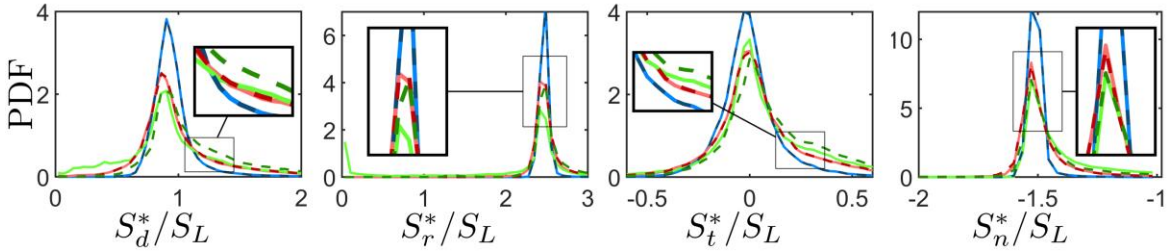

Figure 3: The PDFs of S_d^*/S_L and its components (i.e., S_r^*/S_L, S_n^*/S_L and S_t^*/S_L) for the $c = 0.8$ isosurface for adiabatic (dashed line) and isothermal (solid line) wall conditions at $t/t_f = 3.99$ (blue), 10.92 (red), 13.12 (green)

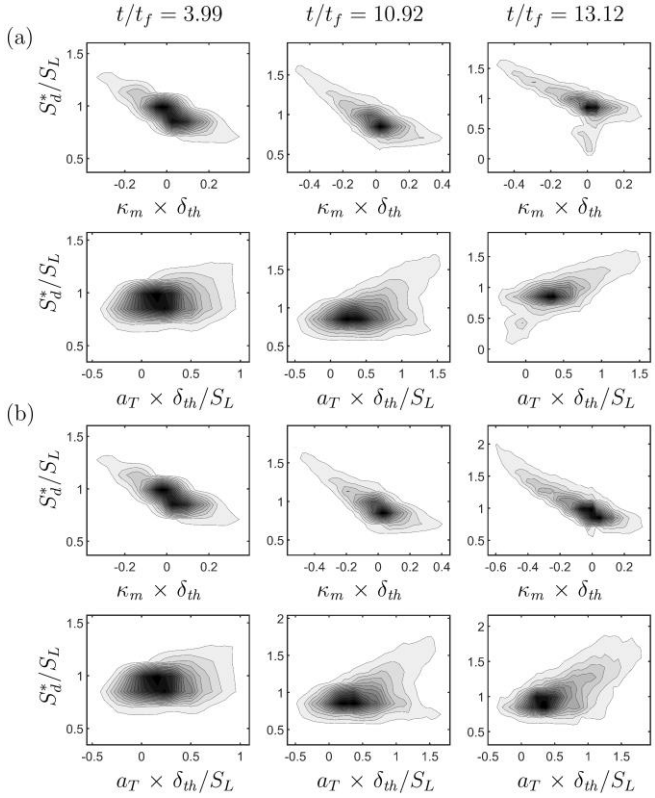

Figure 4: Contours of joint PDFs of S_d^*/S_L with $\kappa_m \times \delta_{th}$ and $a_T \times \delta_{th}/S_L$ for the $c = 0.8$ isosurface for isothermal (a) and adiabatic (b) wall conditions at $t/t_f = 3.99, 10.92$ and 13.12 .

The correlations of S_d^*/S_L with tangential strain rate $a_T = (\delta_{ij} - N_i N_j)\partial u_i/\partial x_j$ and curvature $\kappa_m = 0.5(\partial N_i/\partial x_i)$ for the $c = 0.8$ isosurface at different stages of HOI are shown in Fig. 4. The correlation between S_d^*/S_L and $\kappa_m \times \delta_{th}$ remains negative at all stages of HOI. The qualitative nature of this correlation changes in response to the wall boundary condition at the final stages of HOI (e.g. $t/t_f = 13.12$). It has been found that S_d^*/S_L remains weakly correlated with $a_T \times \delta_{th}/S_L$ at early stage of HOI (e.g. $t/t_f = 3.99$) while the interaction of flame with the wall gives rise to a strong positive correlation at final stage for both wall boundary conditions. This behaviour can be explained through the a_T and κ_m dependences of S_r^*, S_n^* and S_t^*, which will be explained in detail in the full paper.

4 Conclusions

Three-dimensional DNS data of HOI of statistically planar flames with a chemically inert wall across turbulent boundary layers for both isothermal and adiabatic wall boundary conditions have been considered to investigate the statistics of density-weighted displacement speed S_d^* and its components during FWI. The FWI has been found to give rise to a reduction in the mean value of S_d^* and the PDFs of S_d^* have been found to widen with the progress of HOI. Dependencies of displacement speed to flame curvature and tangential strain rate have been found to be significantly affected by the existence of wall and the type of wall boundary condition.

Acknowledgements

The authors are grateful for the financial and computational supports from the Engineering and Physical Sciences Research Council, UK (Grant: EP/V003534/1 and EP/R029369/1).

References

[1] Peters, N., Terhoeven, P., Chen, J.H., Echekki, T. (1998). Statistics of flame displacement speeds from computations of 2-D unsteady methane-air flames, Proc. Combust. Inst., 27:833.

[2] Echekki, T., Chen, J.H., (1999), Analysis of the contribution of curvature to premixed flame propagation, Combust. Flame, 118: 303.

[3] Chakraborty, N., Cant, R.S. (2004). Unsteady effects of strain rate and curvature on turbulent premixed flames in an inflow-outflow configuration, Combust. Flame, 137:129.

[4] Keil, F.B., Amzehnhoff, M., Ahmed, U., Chakraborty, N., Klein, M. (2021). Comparison of flame propagation statistics extracted from DNS based on simple and detailed chemistry Part 1: Fundamental flame turbulence interaction, Energies, 14: 5548.

[5] Peters, N. (2000). Turbulent Combustion, Cambridge Monograph on Mechanics. Cambridge University Press, Cambridge.

[6] Chakraborty, N., Cant, R.S. (2007). A-Priori Analysis of the curvature and propagation terms of the Flame Surface Density transport equation for Large Eddy Simulation. Phys. Fluids, 19:105101.

[7] Ahmed, U., Chakraborty, N., Klein, M. (2021). Scalar gradient and strain rate statistics in oblique premixed flame-wall interaction within turbulent channel flows, Flow, Turb. Combust.,106:701.

[8] Ahmed, U., Chakraborty, N., Klein, M. (2021). Assessment of Bray Moss Libby formulation for premixed flame-wall interaction within turbulent boundary layers: Influence of flow configuration, Combust. Flame, 233:111575.

[9] Ahmed, U., Chakraborty, N., Klein, M. (2021). Influence of thermal wall boundary condition on scalar statistics during flame-wall interaction of premixed combustion in turbulent boundary layers, Int J Heat Fluid Flow, 92: 108881.

[10] Lai, J., Klein, M., Chakraborty, N. (2018). Direct Numerical Simulation of head-on quenching of statistically planar turbulent premixed methane-air flames using a detailed chemical mechanism, Flow, Turb. Combust.,101:1073.

[11] Ahmed, U., Apsley, D., Stallard, T., Stansby, P., Afgan, I. (2021). Turbulent length scales and budgets of Reynolds stress-transport for open-channel flows; friction Reynolds numbers Re_τ=150, 400 and 1020, J. Hydraul. Res., 59:36.